

RESEARCH ARTICLE

Transient time correlation function calculation of the viscosity of a molecular fluid at low shear rates: a comparison of stress tensors

Oleg A. Mazyar, Guoai Pan and Clare McCabe*

Department of Chemical Engineering, Vanderbilt University, Nashville, TN 37235-1604, USA

(Received 2 November 2008; final version received 24 March 2009)

Shear viscosity of *n*-decane was computed using the molecular stress transient time correlation function (TTCF) formalism for the wide range of shear rates from $1.7 \times 10^{10} \text{ s}^{-1}$ to $2.13 \times 10^4 \text{ s}^{-1}$. In earlier work calculations were presented for the shear viscosity of *n*-decane using the atomic stress formalism of the TTCF method (G. Pan and C. McCabe, *J. Chem. Phys.* **125**(19), 4527 (2006)) in which we were able to close the gap between the lowest shear rates accessible by direct nonequilibrium molecular dynamics (NEMD) simulations and the highest shear rates possible in experimental studies. Here it is shown that the application of the molecular stress approach within the TTCF formalism, as an alternative to the atomic stress method, significantly reduces the number of NEMD trajectories necessary to obtain the shear viscosity.

Keywords: transient time correlation function; TTCF; viscosity; alkanes; nonequilibrium molecular dynamics simulation

1. Introduction

Reliable prediction of shear viscosity for molecular fluids subjected to a wide range of strain rates and at different temperature and pressure conditions is of significant theoretical and industrial interest [1–4]. Most fluids exhibit a shear viscosity that is independent of strain rate, yielding the so-called Newtonian plateau viscosity up to a certain critical strain rate $\dot{\gamma} \equiv \partial u_x / \partial y$, where u_x is the streaming velocity in the x direction and y the vertical position, above which the viscosity decreases with increasing strain rate. Such behaviour, known as shear thinning, typically occurs at $\dot{\gamma}_c \approx \tau^{-1}$, where τ is the longest relaxation time in the fluid at equilibrium in the absence of shear and for a molecular fluid is usually the rotational relaxation time (τ_{rot}). With experimentally accessible strain rates limited to around 10^5 s^{-1} and below, this critical strain rate, $\dot{\gamma}_c$, can be accessed only at very high pressures and low temperatures for relatively simple molecular fluids, when their relaxation time τ_{rot} exceeds 10^{-5} s [1].

Alternatively, the shear viscosity for molecular fluids can be predicted in the Newtonian regime by employing computational techniques based on either equilibrium or non-equilibrium molecular dynamics methods (EMD and NEMD, respectively) [2,3]. However these approaches are also not without significant challenges; first, reliable shear viscosity

computations with EMD require simulations lasting at least several hundred relaxation times [5,6], i.e. more than 10^{-3} s , while the length of typical MD trajectory rarely exceeds tens of nanoseconds. Secondly, while the shear viscosity of a fluid can be determined directly from steady-state NEMD methods, such simulations demonstrate poor signal-to-noise ratio at low strain rates and thus, cannot be used for computations of viscosity within the Newtonian plateau [2], accurate determination of which is needed to estimate the extent of the Newtonian plateau and hence $\dot{\gamma}_c$.

In order to close the gap between the lowest shear rates accessible by MD simulations and the highest shear rates possible in experimental studies, another computational approach has to be applied, which is reliable at low shear rates. Morris and Evans [2,7,8] developed the transient-time correlation function (TTCF) technique, which is a nonlinear generalization of the Green–Kubo relations, forming a bridge between the Green–Kubo method (which can be used only at equilibrium) and direct NEMD (which performs efficiently at high strain rates). The TTCF method correlates the fluctuations in a phase variable evaluated at equilibrium, when no external perturbation is applied, and fluctuations in another phase variable during the establishment of nonequilibrium steady state after a perturbation is turned on. Within the TTCF formalism, the shear viscosity is

*Corresponding author. Email: c.mccabe@vanderbilt.edu

obtained by integrating the shear stress autocorrelation function:

$$\langle \eta(t; \dot{\gamma}) \rangle = -\frac{V}{k_B T} \int_0^t ds \langle P_{xy}(s; \dot{\gamma}) P_{xy}(0; \dot{\gamma} = 0) \rangle \quad (1)$$

$$\eta(\dot{\gamma}) = \lim_{t \rightarrow \infty} \langle \eta(t; \dot{\gamma}) \rangle,$$

where V is the volume of the system, T is the temperature, k_B Boltzmann's constant, s the time, and P_{xy} the xy element of the stress tensor computed during the NEMD trajectory ($P_{xy}(s; \dot{\gamma})$) when a strain rate $\dot{\gamma}$ is applied and at the beginning of the trajectory ($P_{xy}(0; \dot{\gamma} = 0)$) when the system is at equilibrium. Note the integral of the average shear stress autocorrelation function over an ensemble of equilibrium initial configurations, $\langle P_{xy}(s; \dot{\gamma}) P_{xy}(0; \dot{\gamma} = 0) \rangle$, in the right side of Equation (1). The shear viscosity at shear rate $\dot{\gamma}$ is the integral of the averaged shear stress autocorrelation function over infinite time. Thus, this method still requires NEMD simulations lasting longer than the relaxation time of the fluid to generate a planar Couette flow; however, in the small shear rate limit, its signal-to-noise ratio becomes equal to that of the equilibrium Green-Kubo technique [2].

The TTCF formalism has been successfully applied by Borzsak and coworkers to compute the shear viscosity of a WCA fluid at the Lennard-Jones triple point over a wide range of strain rates (10^{-7} to 1.44 in reduced units) [9]. It was shown that the TTCF calculations yield viscosity values with the precision of the Green-Kubo method at low shear rates and predict consistent results with the direct steady-state NEMD computations at high shear rates. In a similar approach, Delhommelle and Cummings [10] studied the shear viscosity of a WCA liquid confined to a film of several molecular diameters at low shear rates and Desgranges and Delhommelle [10] have investigated the rheological properties of liquid copper in the Newtonian and shear-thinning regimes using the TTCF method.

Recently, for the first time, the TTCF approach was proven to be an effective method for prediction of the rheological response of a molecular fluid, i.e. n -decane, subjected to the low shear rates accessible by experimental measurements [12]. While the Newtonian and shear-viscosity of decane can be determined from EMD and NEMD simulations, respectively, this work demonstrated that the TTCF method can be used for the accurate prediction of the rheological properties of fluids at realistic operating conditions [1–3]. For a molecular fluid, the stress can be calculated using two different approaches: the atomic and molecular formalisms. In the atomic

formalism, used by Pan and McCabe [12], the stress tensor is computed from coordinates, momenta, and forces acting on individual atoms comprising the molecules in the system:

$$\mathbf{P}^{(a)} V = \sum_{ia} \left(\frac{\mathbf{p}_{ia} \mathbf{p}_{ia}}{m_{ia}} + \mathbf{r}_{ia} \mathbf{F}_{ia} \right), \quad (2)$$

where m_{ia} , \mathbf{p}_{ia} , \mathbf{r}_{ia} , and \mathbf{F}_{ia} are the mass, momentum, coordinates, and the total force acting on atom a in molecule i . Alternatively in the molecular approach, the stress tensor is calculated using positions and momenta of the centre of mass of the molecules in the system as well as total forces acting on the molecules:

$$\mathbf{P}^{(m)} V = \sum_i \left(\frac{\mathbf{p}_i \mathbf{p}_i}{m_i} + \mathbf{r}_i \mathbf{F}_i \right), \quad (3)$$

where m_i , \mathbf{p}_i , \mathbf{r}_i , and \mathbf{F}_i are the mass, centre of mass momentum and coordinates, and the total force acting on molecule i . The equivalence, and difference, of the atomic and molecular formalisms for the pressure tensor has been discussed significantly in the literature (see, for example, [5,13–17]). The equivalence of the two formalisms for pressure in the thermodynamic limit has been shown in several studies [13,14,17]. For example, Akkermans and Ciccotti [14] showed that under periodic boundary conditions, the atomic and molecular stress tensor expressions are equivalent, while in a closed system, the difference between them vanishes in the thermodynamic limit. Of particular relevance to the current work, Maréchal and Rycakert [17] showed that the transport coefficients obtained from the two formalisms are the same in the long time limit, while the difference in partial integrals of stress auto-correlation functions involves a slow decay proportional to $t^{-1/2}$. Subsequently, Allen [15] explicitly showed that the two formalisms for the stress tensors of multi-atomic molecules differ by a term involving the second derivative of an orientation tensor θ ,

$$\mathbf{P}^{(a)} = \mathbf{P}^{(m)} + \frac{1}{2} \ddot{\theta} \quad (4)$$

where

$$\theta = \sum_{ia} m_{ia} \delta \mathbf{r}_{ia} \delta \mathbf{r}_{ia} \quad (5)$$

here $\mathbf{P}^{(a)}$ in Equation (4) is the atomic stress tensor, $\mathbf{P}^{(m)}$ the symmetric part of the molecular stress tensor, and m_{ia} and $\delta \mathbf{r}_{ia}$ are the mass and position vector of atom a in molecule i from the center of mass of the molecule. Therefore, the relationship between the

atomic and molecular forms of the stress-stress autocorrelation function can be written as:

$$\begin{aligned} \left\langle P_{\alpha\beta}^{(a)}(t)P_{\alpha\beta}^{(a)}(0) \right\rangle &= \left\langle P_{\alpha\beta}^{(m)}(t)P_{\alpha\beta}^{(m)}(0) \right\rangle + \left\langle \ddot{\theta}_{\alpha\beta}(t)P_{\alpha\beta}^{(m)}(0) \right\rangle \\ &+ \frac{1}{4} \left\langle \ddot{\theta}_{\alpha\beta}(t)\ddot{\theta}_{\alpha\beta}(0) \right\rangle \end{aligned} \quad (6)$$

where $P_{\alpha\beta}^{(a)}$ and $P_{\alpha\beta}^{(m)}$ are the elements of the atomic stress tensor and the symmetrized molecular stress tensor, respectively [4,16]. Cui *et al.* [16,18] fully examined the differences between the atomic and molecular formalisms in EMD simulations of *n*-decane, at the same state point as considered in the current work, and found that the first and second terms on the right-hand side of Equation (6) are small compared with the third term, and that the second term decays to zero faster than the third term (~ 0.5 ps compared with ~ 3 ps). Furthermore, the viscosities calculated in the EMD simulations through the Green–Kubo formula using the atomic and molecular stress autocorrelation functions were found to be equivalent. Mondello and Grest [5] also achieved consistent results from Green–Kubo calculations for the viscosity of *n*-hexadecane using the two formalisms.

In this work, we examine the use of both atomic and molecular formalisms for computing the stress tensor in the TTCF calculations of shear viscosity of a molecular fluid. While the use of the molecular and atomic stress tensors has been fully probed in NEMD simulations, as discussed above, this has not yet been addressed in TTCF calculations.

2. Computational procedure

The motion of *n*-decane molecules in planar Couette shear flow is described by the SLLOD equations [2] combined with Lees–Edwards shearing periodic boundary conditions and a Gaussian thermostat:

$$\begin{aligned} \frac{d\mathbf{r}_i}{dt} &= \frac{\mathbf{p}_i}{m_i} + \dot{\gamma}y_i\hat{\mathbf{x}} \\ \frac{d\mathbf{p}_i}{dt} &= \mathbf{F}_i - \dot{\gamma}p_{y,i}\hat{\mathbf{x}} - \alpha\mathbf{p}_i \end{aligned} \quad (7)$$

where $\mathbf{r} = (x, y, z)$ and $\mathbf{p} = (p_x, p_y, p_z)$ are the particle coordinates and momenta, $\dot{\gamma}$ is the shear rate, and $\hat{\mathbf{x}}$ is a unit vector in the *x* direction and \mathbf{F}_i the force acting on particle *i*. The Gaussian thermostating [19] multiplier α is computed by ensuring that $(d/dt) \sum_i (\mathbf{p}_i^2/2m_i) = 0$ at each time step:

$$\alpha = \frac{\sum_i (\mathbf{F}_i \cdot (\mathbf{p}_i/m_i) - \dot{\gamma}p_{x,i}p_{y,i}/m_i)}{\sum_i (\mathbf{p}_i^2/m_i)}. \quad (8)$$

To avoid a kinetic energy drift observed when a conventional integrator is used to integrate the Gaussian thermostatted SLLOD equations, a novel multiple time step method coupled with a Gaussian thermostat [19] and operator splitting algorithm, that achieves strict kinetic energy control and was developed by Pan *et al.* [12] is used. The choice of the thermostat is motivated by the fact that the Gaussian thermostat does not require an empirical relaxation time for temperature control, which is an important property for the transient NEMD simulations performed in the TTCF method. Thus, the MD simulations were performed in the isothermal-isochoic ensemble. Note that Equations (7) and (8) based on the atomic SSLOD algorithm are applied to the molecular system and as such are not rigorously correct, as shown by Travis *et al.* [20,21]. This is because a molecular fluid in a shear field undergoes shear-induced rotational motion that should be subtracted from the rotational velocity to determine the peculiar rotational motion that can then be thermostatted [22]. Applying an atomic thermostat, as given above, does not in principle achieve this goal. As shown by Lue *et al.* [23], one can instead thermostat only the center-of-mass motion, however, this leads to more complicated equations of motion. To overcome this limitation, Evans and co-workers showed how configurational expressions for the thermodynamic temperature can be used to develop a thermostat that avoids the problems encountered with the use of either centre of mass or atomic thermostats for molecular fluids [24,25] and Travis and Braga [26] recently proposed a new configurational thermostat which has been applied by Desgranges and Delhommelle [27] to determine the conductivity of a model confined fluid using the TTCF approach. Since differences in viscosity between rigorously thermostatted systems and the atomic thermostat (as used in this work) are evident only in the non-linear response regime (reduced strain rate $O(1)$ and higher), our results (which are for strain rates of 0.04 and less) are essentially unaffected by the atomic thermostat used. Additional evidence for this conclusion is given by Travis *et al.*, who saw differences between atomic and rigorously thermostatted systems for eicosane only above shear rates of unity [21] and Delhommelle and Evans, who noted for decane and eicosane that the results obtained using either a configurational or center of mass thermostat were identical at low shear rates (reduced strain rates less than 0.5) [25].

For consistency, and to allow a direct comparison of our results with those presented in earlier work, *n*-decane is modeled by the SKS united atom (UA) force field proposed by Siepmann and

co-workers [28,29], with the modification that the fixed bonds are replaced by a stiff harmonic bond stretching potential in order to generate a fully flexible model [12,18,30]. In the UA model, the CH₃ and CH₂ groups are coarse-grained into single spherical interaction sites with the interaction center located at the center of each carbon atom. The intramolecular interactions are described by harmonic bond stretching, harmonic valence angle bending [28], and torsional potentials [31]. The intermolecular interactions and the interactions between united atoms separated by three or more bonds in the same molecule are represented by Lennard–Jones potentials. Lorentz–Berthelot combining rules were used to determine the cross or unlike interactions and a cutoff distance of $2.5\sigma_0$ (9.825 Å) was used, where $\sigma_0 = 3.93$ Å and corresponds to the diameter of the CH₂ united atom site. Full details of the model are given in the original papers [28–30].

As in our earlier work [11], on the viscosity of *n*-decane using TTCF of the atomic stress tensor, the simulations were carried out on 100 *n*-decane molecules at 480 K and a density of 0.6136 g/cm³. A time step size of 2.35 fs was used for slow motions and a sub-time step size of 0.235 fs for the fast motions in the multiple time step method. Note that using the characteristic energy and length scales of a CH₂ group, 1 unit of dimensionless time, which is given by $\sqrt{m\sigma^2/\varepsilon}$, is 2.35 ps. Hence, the time steps used correspond to 10^{-3} and 10^{-4} in dimensionless time units.

The equilibration of the system was carried out following Cui *et al.* [18]. The molecules were placed in the simulation box with their center of mass at lattice points in the all trans conformation. The LJ interaction was grown from $0.05\sigma_0$ to σ_0 in a 20,000 time step initialization period during which rescaling of the velocities was performed. Velocity rescaling was continued for a further 110,000 time steps, followed by an additional 4.2×10^5 time steps (~ 1 ns) of Gaussian thermostatted equilibration. After the equilibration, the MD simulations were run for an additional ~ 20 ns to generate 18,000 equilibrated configurations, which serve as starting configurations for the TTCF calculations. The equilibrated configurations were saved every 500 time steps to ensure that these configurations were uncorrelated. Since the length of NEMD trajectories for the TTCF computations must be greater than the characteristic time required for the molecular fluid to reach a steady state, i.e. the molecular orientation relaxation time of *n*-decane, we performed simulations at six different shear rates using the following number of time steps for the transient period; 7,000 time steps (16.45 ps)

were used for $\dot{\gamma} = 0.04 (1.7 \times 10^{10} \text{ s}^{-1})$ and $\dot{\gamma} = 5 \times 10^{-4} (2.13 \times 10^8 \text{ s}^{-1})$ and 10,000 time steps (23.5 ps) were used for the lower shear rates, $\dot{\gamma} = 5 \times 10^{-5} (2.13 \times 10^7 \text{ s}^{-1})$, $\dot{\gamma} = 5 \times 10^{-6} (2.13 \times 10^6 \text{ s}^{-1})$, $\dot{\gamma} = 5 \times 10^{-7} (2.13 \times 10^5 \text{ s}^{-1})$, and $\dot{\gamma} = 5 \times 10^{-8} (2.13 \times 10^4 \text{ s}^{-1})$ [11]. The TTCF technique was also tested at its asymptotic conditions, i.e. at the shear rate of $\dot{\gamma} = 0.0$. In this simulation, 10,000 steps were used for the ‘transient’ period.

As the ensemble-averaged autocorrelation function $\langle P_{xy}(s; \dot{\gamma}) P_{xy}(0; \dot{\gamma} = 0) \rangle$ approaches $\langle P_{xy}(s; \dot{\gamma}) \rangle \langle P_{xy}(0; \dot{\gamma} = 0) \rangle$ as the time $s \rightarrow \infty$, it is necessary to choose equilibrium starting states Γ in such a way that $\langle P_{xy}(0; \dot{\gamma} = 0) \rangle \equiv 0$ to minimize the statistical uncertainties in the transient correlation integral in Equation (1). This is achieved through trajectory mapping [2,8], which generates three additional starting configurations from the initial configuration $\Gamma = (x, y, z, p_x, p_y, p_z)$ that occur within the equilibrium distribution of states with the same probability as Γ . For each Γ , four mapped configurations

$$\begin{aligned} \Gamma^J &= (x, y, z, p_x, p_y, p_z) \\ \Gamma^T &= (x, y, z, -p_x, -p_y, -p_z) \\ \Gamma^Y &= (x, -y, z, p_x, -p_y, p_z) \\ \Gamma^K &= (x, -y, z, -p_x, p_y, -p_z) \end{aligned} \quad (9)$$

lead to four different trajectories with the initial shear stress equal to $P_{xy}(0)$ for Γ^J and Γ^T configurations and $-P_{xy}(0)$ for Γ^Y and Γ^K configurations. Thus, the sum of the shear stresses for the four starting configurations is exactly 0. This eliminates the statistical difficulties associated with the small, yet nonzero, value of $\langle P_{xy}(0) \rangle$ at long times and establishes the trajectory mapping technique as a central part of the TTCF method.

During the NEMD computations, the stress tensor was evaluated using both the atomic and molecular formalism as given by Equation (2) and Equation (3), respectively, and the shear stress autocorrelation function $\langle P_{xy}(s; \dot{\gamma}) P_{xy}(0; \dot{\gamma} = 0) \rangle$ in Equation (1) was averaged over $4 \times 18,000$ configurations (where 4 indicates the 4 new starting configurations derived using the trajectory mapping technique).

3. Results and discussion

The TTCF calculations were performed with correlation functions for both the atomic shear stress and molecular shear stress for comparison. As can be seen in Figure 1, where we present the transient time correlation functions for *n*-decane at a shear rate of

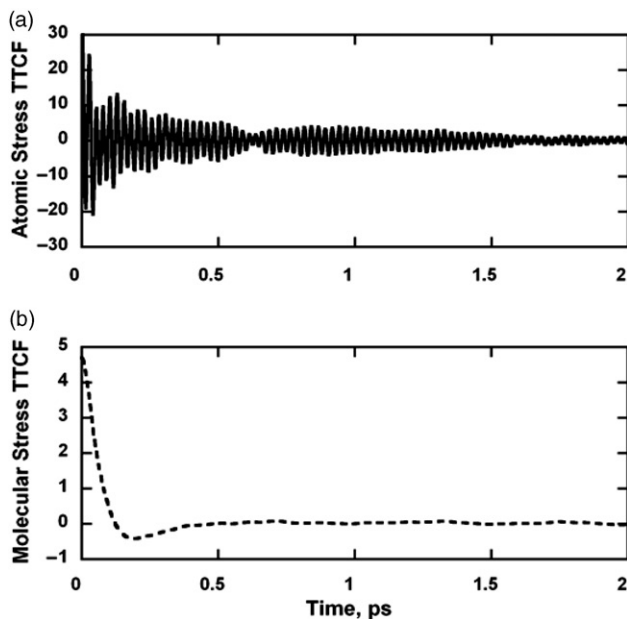


Figure 1. Transient time correlation functions of shear stresses from (a) atomic and (b) molecular formalisms at a reduced shear rate of 0.0005.

$\dot{\gamma} = 5 \times 10^{-4}$ ($2.13 \times 10^8 \text{ s}^{-1}$), the atomic and molecular formalisms show different responses in the relaxation of the transient process. The atomic shear stress correlation function exhibits strong oscillatory behavior [12] while the molecular shear stress correlation function initially decays and reaches its minimum at ~ 0.2 ps and then increases to zero exhibiting long-time noise. We note that the period of the oscillation of the atomic shear stress correlation function is 0.023 ps, which is a fraction (10^{-2}) of the characteristic time unit in the UA model (2.35 ps) and corresponds to the harmonic bond stretching. This illustrates the need to carefully select the time intervals at which to evaluate atomic stress correlation functions, in order to avoid missing the true oscillatory behavior; failure to take this into account can lead to inaccurate values for the viscosity. The strong oscillation in the atomic shear stress transient time correlation functions leads to much noisier viscosity curves computed from the transient correlation integral in Equation (1) compared with those obtained from the molecular shear stress correlation functions, as displayed in Figure 2. While averaging of the molecular shear stress autocorrelation function $\langle P_{xy}(s; \dot{\gamma}) P_{xy}(0; \dot{\gamma} = 0) \rangle$ over $4 \times 18,000$ configurations results in viscosity curves reaching a plateau after 8 ps as shown in Figure 2(b), this number of configurations was found to be insufficient for computing accurate viscosities from atomic shear stress correlation functions below shear rates of $\dot{\gamma} = 5 \times 10^{-5}$ ($2.13 \times 10^7 \text{ s}^{-1}$) [12]. For the same

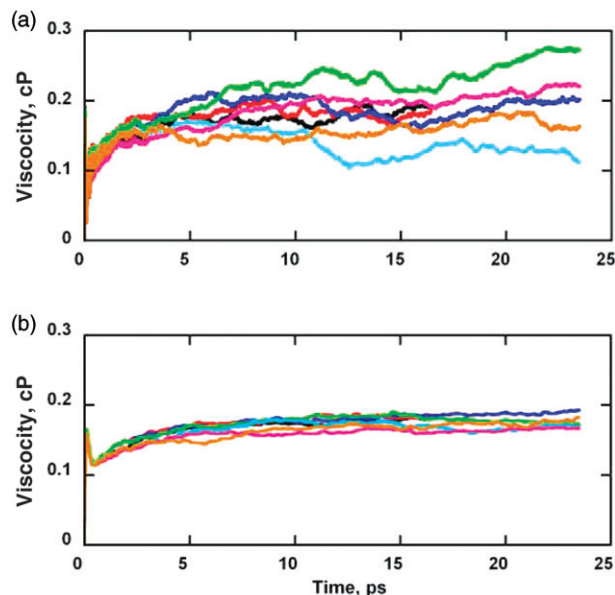


Figure 2. (Colour online). TTCF calculated viscosities from (a) the atomic shear stress correlation and (b) the molecular shear stress correlation, at various shear rates in transient states. The curves shown correspond to the following shear rates, $\dot{\gamma}$: magenta $\dot{\gamma} = 5 \times 10^{-8}$; light blue $\dot{\gamma} = 5 \times 10^{-7}$; green $\dot{\gamma} = 5 \times 10^{-6}$; blue $\dot{\gamma} = 5 \times 10^{-5}$; red $\dot{\gamma} = 5 \times 10^{-4}$; black $\dot{\gamma} = 4 \times 10^{-2}$; brown $\dot{\gamma} = 0$.

system, Pan *et al.* [11] used averaging over $4 \times 30,000$ configurations in order to obtain converging viscosity curves from the atomic shear stress correlation functions. In Table 1, viscosities from the transient atomic and molecular stress correlation integrals are reported for comparison. For higher shear rates of $\dot{\gamma} \geq 5 \times 10^{-6}$ ($2.13 \times 10^6 \text{ s}^{-1}$), viscosities computed using both molecular and atomic stress formalisms are in good agreement; however, a discrepancy between the viscosities from the molecular and atomic stress tensors, 0.169 ± 0.016 versus 0.182 ± 0.007 cP, respectively, is observed for the lowest shear rate $\dot{\gamma} = 5 \times 10^{-7}$ ($2.13 \times 10^5 \text{ s}^{-1}$) considered by Pan *et al.* [12], although these two values still agree within error limits. Relatively high errors for the viscosities computed from the atomic shear stress correlation integrals based on averaging over $4 \times 18,000$ configurations makes the comparison of viscosities from the atomic and molecular stress tensors somewhat problematic at shear rates $\dot{\gamma} = 5 \times 10^{-8}$ ($2.13 \times 10^4 \text{ s}^{-1}$) and $\dot{\gamma} = 0.0$, and clearly indicates an advantage of using the molecular versus the atomic pressure formalism in the TTCF computations (see Table 1). This result is in agreement with the work of Gordon [5], who for EMD viscosity calculations found the pressure computed with the molecular formalism for fully flexible molecular models of liquid *n*-octane and *n*-dodecane to be more robust than the atomic pressure

Table 1. Viscosities of *n*-decane predicted from TTCF calculations at various shear rates using both the atomic stress and molecular stress correlations.

Reduced shear rate	Shear rate, s ⁻¹	Atomic viscosity, cP	Molecular viscosity, cP
0.0	0.0	0.164 ± 0.037	0.172 ± 0.016
0.00000005	2.13 × 10 ⁴	0.205 ± 0.040	0.164 ± 0.009
0.0000005	2.13 × 10 ⁵	0.182 ± 0.007 ^a	0.169 ± 0.016
0.000005	2.13 × 10 ⁶	0.176 ± 0.014 ^a	0.180 ± 0.010
0.00005	2.13 × 10 ⁷	0.186 ± 0.008 ^a	0.186 ± 0.015
0.0005	2.13 × 10 ⁸	0.182 ± 0.009 ^a	0.182 ± 0.015
0.04	1.70 × 10 ¹⁰	0.178 ± 0.013 ^a	0.176 ± 0.015

^aViscosities reported by Pan *et al.* [12].

and displayed no dependence on the magnitude of the time step employed in the integration scheme [5]. This observation differs from the finding of Mondello and Grest [6] who for a fixed-bond model of *n*-alkanes found the atomic pressure to be much less sensitive to details of the integration method. This is perhaps not surprising, given that a fixed bond model will not exhibit the rapid oscillations seen in Figure 1(a), since the oscillations originate in the intramolecular vibrational motions. We also note from Table 1 that at shear rates $\dot{\gamma} \leq 5 \times 10^{-7}$ ($2.13 \times 10^5 \text{ s}^{-1}$), the viscosities computed using the molecular stress tensor are 5–9% lower than those obtained for the higher shear rates using the TTCF technique; although, again, the viscosities obtained from the molecular stress tensor agree within their error limits over six orders of magnitude in shear rate.

4. Conclusions

Nonequilibrium molecular dynamic simulations were performed and the shear viscosity of *n*-decane calculated for the wide range of the shear rates from $\dot{\gamma} = 0.04$ ($1.7 \times 10^{10} \text{ s}^{-1}$) to $\dot{\gamma} = 5 \times 10^{-8}$ ($2.13 \times 10^4 \text{ s}^{-1}$) using the molecular stress TTCF formalism. It was shown that the application of the molecular stress approach within the TTCF formalism, as an alternative to the atomic stress method, significantly reduces the number of NEMD trajectories necessary to obtain converging values for the shear viscosity. One possible explanation for this is that the molecular velocity profile is expected to be closer to the assumed Couette linear profile ($u_x = \dot{\gamma}y$) than the atomic velocity profile; the larger deviations from the linearity for the atomic velocity profile are thus the likely source of the additional noise seen in Figure 2. At the lowest shear rates studied ($10^4 - 10^5 \text{ s}^{-1}$), the TTCF method brings the molecular simulations into the range of experimentally accessible shear rates. Therefore, the TTCF technique enables us to study the transport properties of systems in which shear

thinning occurs at shear rates lower than those reachable by NEMD but higher than the experimentally accessible range and can be used to bridge the gap between the NEMD and Green–Kubo calculations.

Acknowledgement

This work was supported by the Office of Naval Research under grant number N00014-06-1-0624. CMC also acknowledges the Jacob Wallenberg Foundation.

References

- [1] S. Bair, C. McCabe, and P.T. Cummings, *Phys. Rev. Lett.* **88**(5), 058302 (2002).
- [2] D.J. Evans and G.P. Morriss, *Statistical Mechanics of Nonequilibrium Liquids* (Academic Press, New York, 1990).
- [3] S.S. Sarman, D.J. Evans, and P.T. Cummings, *Phys. Rep. – Rev. Section Phys. Lett.* **305**(1–2), 1 (1998).
- [4] P.A. Gordon, *Ind. Eng. Chem. Res.* **42**, 7025 (2003).
- [5] P.A. Gordon, *Mol. Simulation* **29**(8), 479 (2003).
- [6] M. Mondello and G.S. Grest, *J. Chem. Phys.* **106**(22), 9327 (1997).
- [7] D.J. Evans and G.P. Morriss, *Phys. Rev. A* **38**(8), 4142 (1988).
- [8] G.P. Morriss and D.J. Evans, *Phys. Rev. A* **35**(2), 792 (1987).
- [9] I. Borzsak, P.T. Cummings, and D.J. Evans, *Mol. Phys.* **100**(16), 2735 (2002).
- [10] J. Delhommelle and P.T. Cummings, *Phys. Rev. B* **72**(17), 2201 (2005).
- [11] C. Desgranges and J. Delhommelle, *J. Chem. Phys.* **128**, 084506 (2008).
- [12] G. Pan and C. McCabe, *J. Chem. Phys.* **125**(19), 4527 (2006).
- [13] R.L.C. Akkermans and W.J. Briels, *J. Chem. Phys.* **114**(2), 1020 (2001); G. Ciccotti and J.P. Ryckaert, *Comput. Phys. Rep.* **4**(6), 345 (1986); W.K. den Otter, M. Krohn and J.H.R. Clarke, *Phys. Rev. E* **65**(1), 6704 (2002).
- [14] R.L.C. Akkermans and G. Ciccotti, *J. Phys. Chem. B* **108**(21), 6866 (2004).

- [15] M.P. Allen, *Mol. Phys.* **52**(3), 705 (1984).
- [16] S.T. Cui, P.T. Cummings, and H.D. Cochran, *Mol. Phys.* **88**(6), 1657 (1996).
- [17] G. Marechal and J.P. Ryckaert, *Chem. Phys. Lett.* **101**(6), 548 (1983).
- [18] S.T. Cui, P.T. Cummings, and H.D. Cochran, *J. Chem. Phys.* **104**(1), 255 (1996).
- [19] M.E. Tuckerman, C.J. Mundy, and G.J. Martyna, *Europhys. Lett.* **45**(2), 149 (1999).
- [20] K.P. Travis, P.J. Daivis and D.J. Evans, *J. Chem. Phys.* **103**(3), 1109 (1995); K.P. Travis, P.J. Daivis and D.J. Evans, *J. Chem. Phys.* **103**(24), 10638 (1995); K.P. Travis, P.J. Daivis and D.J. Evans, *J. Chem. Phys.* **105**(9), 3893 (1996).
- [21] K.P. Travis and D.J. Evans, *Mol. Simulation* **17**, 157 (1996).
- [22] K.P. Travis and D.J. Evans, *Phys. Rev. E* **55**(2), 1566 (1997); J. Delhommelle and D.J. Evans, *Mol. Phys.* **100**(17), 2857 (2002).
- [23] L. Lue, O.G. Jepps, J. Delhommelle, and D.J. Evans, *Mol. Phys.* **100**(14), 2387 (2002).
- [24] J. Delhommelle and D.J. Evans, *J. Chem. Phys.* **115**(1), 43 (2001).
- [25] J. Delhommelle and D.J. Evans, *J. Chem. Phys.* **117**(13), 6016 (2002).
- [26] K.P. Travis and C. Braga, *J. Chem. Phys.* **128**(1), 10 (2008).
- [27] C. Desgranges and J. Delhommelle, *Phys. Rev. E* **77**(2), 4 (2008).
- [28] J.I. Siepmann, S. Karaborni, and B. Smit, *J. Am. Chem. Soc.* **115**(14), 6454 (1993).
- [29] J.I. Siepmann, S. Karaborni, and B. Smit, *Nature* **365**(6444), 330 (1993); B. Smit, S. Karaborni and J.I. Siepmann, *J. Chem. Phys.* **102**(5), 2126 (1995).
- [30] C.J. Mundy, J.I. Siepmann, and M.L. Klein, *J. Chem. Phys.* **102**(8), 3376 (1995).
- [31] W.L. Jorgensen, J.D. Madura, and C.J. Swenson, *J. Am. Chem. Soc.* **106**(22), 6638 (1984).